Identifying the cellular origin of squamous skin tumors

Gaëlle Lapouge[a,1], Khalil Kass Youssef[a,1], Benoit Vokaer[b], Younes Achouri[c], Cindy Michaux[a], Panagiota A. Sotiropoulou[a], and Cédric Blanpain[a,2]

[a]Institut de Recherche Interdisciplinaire en Biologie Humaine et Moléculaire, Université Libre de Bruxelles, B-1070 Brussels, Belgium; [b]Institut d'Immunologie Médicale, Université Libre de Bruxelles, B-6041 Charleroi, Belgium; and [c]Université Catholique de Louvain de Duve Institute, B-1200 Brussels, Belgium

Edited by Brigid L. M. Hogan, Duke University Medical Center, Durham, NC, and approved February 25, 2011 (received for review September 9, 2010)

Squamous cell carcinoma (SCC) is the second most frequent skin cancer. The cellular origin of SCC remains controversial. Here, we used mouse genetics to determine the epidermal cell lineages at the origin of SCC. Using mice conditionally expressing a constitutively active KRas mutant (G12D) and an inducible CRE recombinase in different epidermal lineages, we activated Ras signaling in different cellular compartments of the skin epidermis and determined from which epidermal compartments Ras activation induces squamous tumor formation. Expression of mutant KRas in hair follicle bulge stem cells (SCs) and their immediate progeny (hair germ and outer root sheath), but not in their transient amplifying matrix cells, led to benign squamous skin tumor (papilloma). Expression of $KRas^{G12D}$ in interfollicular epidermis also led to papilloma formation, demonstrating that squamous tumor initiation is not restricted to the hair follicle lineages. Whereas no malignant tumor was observed after $KRas^{G12D}$ expression alone, expression of $KRas^{G12D}$ combined with the loss of p53 induced invasive SCC. Our studies demonstrate that different epidermal lineages including bulge SC are competent to initiate papilloma formation and that multiple genetic hits in the context of oncogenic KRas are required for the development of invasive SCC.

cancer cell of origin | hair follicle stem cells

Squamous cell carcinoma (SCC) is one of two most frequent skin cancers and occurs most frequently in the sun-exposed regions of the skin and in immunocompromised patients. Approximately 250,000 patients per year develop skin SCC in the United States. Although skin SCC is often cured by surgical excision, ≈8% of patients with skin SCC relapse, and 5% present metastasis within 5 y. In patients with metastatic SCC, the prognosis is very poor, with only a 10–20% survival rate over 10 years (1). A better understanding of the early steps of SCC initiation is thus warranted.

The most extensively used mouse cancer model for skin SCC is a multistage chemically induced carcinogenesis (2). In the first step, called initiation, mice are treated with a low dose of the mutagen 9,10-dimethyl-1,2-benzanthracene (DMBA). In the second step, called promotion, mice are treated continuously with a drug that stimulates epidermal proliferation, such as 12-*O*-tetradecanoyl phorbol-13-acetate (TPA). During promotion, benign tumors (papillomas) arise, probably as a consequence of additional mutations, some of which will progress into invasive SCC. Interestingly, using this protocol, papillomas contain activating mutations in *HRas* gene, suggesting that this mutation confers a selective advantage to epithelial cells (3). However, not all papillomas contain mutations in the *HRas* gene, and some papillomas and SCC in both mouse and human present mutations in the *KRas* gene instead (4–6). Whereas *Ras* mutations seem to be an early step in skin cancer initiation, *p53* mutations are associated with malignant progression (7, 8), although a recent report suggests that gain of p53 function increases tumor initiation and progression compared with p53 loss of function (9).

Conflicting results have been reported regarding the determination of which epidermal lineages give rise to squamous cutaneous cancers. The skin epidermis contains different compartments, including the hair follicle (HF) and the sebaceous gland (SG), as well as the interfollicular epidermis (IFE), which are maintained during homeostasis by different types of stem cells (SCs) (10). In the absence of injury, bulge SCs mediate HF regeneration (11–14), whereas the isthmus SCs mediate SG homeostasis (15–17). The maintenance of the IFE is ensured by the juxtaposition of many small epidermal proliferative units containing long-lived progenitors (18, 19). Upon wounding, bulge and isthmus SCs migrate upward and contribute to the repair of the IFE (11, 13, 17, 20). SCCs often present signs of squamous differentiation, as illustrated by the keratin pearls found in the center of the tumors, suggesting that SCCs may originate from the IFE (8). TPA administration stimulates papilloma formation even when TPA administration is started 1 y after the last DMBA treatment, suggesting that the initial mutation arises in long-lived SCs (21). There is some evidence that cells targeted by the benzo (*a*)pyrene or DMBA in the skin can be slow-cycling cells residing in the HF but also along the IFE (21–23). Dermabrasion techniques can selectively remove the IFE while leaving intact HFs, which then contribute to the repair of wounded skin. When TPA is applied after the repair of the epidermis, papilloma formation is reduced but the formation of SCC is not abolished, suggesting that initiating cells may reside in the IFE as well as in HFs (24). However, some studies suggested that oncogenic mutations could also occur in differentiated cells of the epidermis. For example, suprabasal expression of α6β4 integrins can increase the frequency of papillomas after DMBA-TPA treatment (25). In addition, transgenic mice expressing a mutated form of HRas under the promoter of *K10*, a marker of the committed suprabasal cells of the IFE, develop papillomas at sites of wounding (26). Transgenic mice expressing the same oncogene under the control of a truncated form of the *K5* promoter, which is expressed preferentially in the HFs of adult mice, develop papillomas and SCCs (27). In addition, these studies used transgenic mice expressing Ras mutant constitutively from embryonic development to adulthood and at supraphysiological level, leaving open the question of which cells of the skin epidermis are competent to give rise to SCCs upon mutated Ras expression at a physiological level in adult mice.

To determine which epidermal compartments are competent to initiate squamous tumors, we used mouse genetics to assess the incidence of skin cancer after the expression of oncogenic KRas at a physiological level in different epidermal compartments. To avoid the drawback of transgenic approaches that result in the random integration of several copies of the oncogene into differently accessible chromatin regions, we used a genetic mouse model to specifically activate a constitutively active mutant of *KRas* (G12D) knocked in into its own locus ($KRas^{LSL\text{-}G12D}$). Expression of this mutant KRas induced a broad variety of Ras-induced neoplasia (28), including oral (29) and skin (9) squamous tumors. The oncogene is only expressed when the Lox-STOP-Lox

Author contributions: G.L., K.K.Y., and C.B. designed research; G.L., K.K.Y., B.V., Y.A., C.M., and P.A.S. performed research; G.L., K.K.Y., and C.B. analyzed data; and G.L., K.K.Y., and C.B. wrote the paper.

The authors declare no conflict of interest.

This article is a PNAS Direct Submission.

[1]G.L. and K.K.Y. contributed equally to this work.

[2]To whom correspondence should be addressed. E-mail: Cedric.blanpain@ulb.ac.be.

This article contains supporting information online at www.pnas.org/lookup/suppl/doi:10.1073/pnas.1012720108/-/DCSupplemental.

(LSL) cassette is removed by a CRE recombinase. A short course of tamoxifen (TAM) administration in mice expressing CREER leads to a mosaic expression of $KRas^{G12D}$ in the epidermal compartments expressing the CREER, mimicking the natural occurrence of sporadic tumors.

Results

$KRas^{G12D}$ Expression in Bulge SCs and Their HF Progeny Induces Papilloma Formation. We first induced the expression of $KRas^{G12D}$ in bulge SCs and their progeny using mice expressing inducible CRE under the regulatory region of HF-specific promoter [K15-CREPR (12) and K19CREER (30)]. We did observe some leakiness in the K15CREPR/RosaYFP mice, visible by the presence of patches of YFP-expressing cells in the absence of RU486 (Fig. S1 *A* and *B*), whereas no leakiness was detected in the K19CREER/RosaYFP mice (Fig. 1 *A* and *B*) (31). Administration of RU486 in K15CREPR/Rosa-YFP mice induced the expression of YFP mostly in bulge SCs, hair germ (HG), and outer root sheath (ORS) cells but also to a lesser extent in the isthmus, infundibulum (the region that connects the bulge to the IFE) and the IFE (Fig. S1 *C–G*), as previously described (12). TAM administration in K19CREER/RosaYFP mice resulted in the labeling of bulge SCs and their HF progeny (Fig. 1 *C–G*). After TAM administration in K19CREER/$KRas^{G12D}$ mice, recombination of *$KRas^{G12D}$* allele was detected in bulge SCs (α6HCD34H) but not in a6HCD34$^-$ cells (Fig. S2*A*), suggesting that the recombination of *KRas* allele is restricted to the same cells labeled with the RosaYFP. In the K19CREER/$KRas^{LSL\text{-}G12D}$, the expression of the $KRas^{G12D}$ oncogene in bulge SCs and their progeny led to a transient increase in bulge SC proliferation (Fig. S2*B*) and the enlargement of the majority of SGs 1 mo after TAM administration (Fig. S2*C*). These SGs became hyperproliferative, as shown by the increased number of Ki67-positive cells and the expression of K6 (Figs. S1–S3), although they were still able to undergo terminal differentiation, as shown by the presence of sebum (Figs. S1 and S3). The defect in SG homeostasis also led to the formation of cystic structures (Figs. S1 and S3). The SG hyperplasia observed here is reminiscent of the phenotype observed after c-Myc (32) and Δ*N*-Lef1 overexpression (33) or Blimp1 deletion (34) in the skin epidermis. Occasionally, the IFE was also abnormal after $KRas^{G12D}$ expression, as shown by the hyperthickening of the IFE located at the orifice of some abnormal HF with hypertrophic SGs (Figs. S1 and S3). In addition to sebaceous cysts, $KRas^{G12D}$ expression in bulge SCs and their progeny also led to the enlargement and abnormal differentiation of HF and to cystic structures negative for Oil-Red-O staining (Figs. S1 and S3). Altogether, these data show that $KRas^{G12D}$ expression in bulge SCs and their HF progeny led to frequent histological abnormalities, indicating that the majority of HFs expressing mutant KRas developed pathologic features including SG hyperplasia and dysplasia, as well as hyperplasia and aberrant differentiation of the lower HF, some of which degenerated into cystic structures.

To investigate why KRas expression in HF cells induces SG alterations, we performed lineage tracing together with KRas expression (K19CREER/$KRas^{LSL\text{-}G12D}$/RosaYFP mice). Already at 2 wk after TAM administration, more YFP-positive cells were seen in the SG progenitors compared with wild-type mice (Fig. S4*A*). At 4 wk after TAM administration, some YFP-positive cells were detected in hyperplastic SG and sometimes even in the IFE of KRas/YFP mice, whereas no YFP-positive were cells were observed in the SG or the IFE of control mice (K19CREER/RosaYFP mice) (Fig. S4*B*). These findings suggested that $KRas^{G12D}$ expression induces migration of bulge SCs toward the SG and the IFE. However, because there is not a perfect correlation between the hyperplastic phenotype and the YFP expression, our data cannot rule out that KRas expression in HF cells promotes epidermal proliferation by a noncellular autonomous mechanism, and thereby promotes tumorigenesis as it occurs after *Notch1* deletion in the skin epidermis (35).

Tumors arose in the lips (57% of the animals treated), face (35%), and back skin (14%) of K15CREPR/$KRas^{LSL\text{-}G12D}$ mice (n = 14) 2–4 mo after RU486 administration (Fig. S1). Similarly, tumors also arose with similar latency and frequency in the lips (78% of the mice treated) and back skin (33%) of K19CREER/$KRas^{LSL\text{-}G12D}$ mice (n = 9) after TAM administration (Fig. 1 *H* and *K*). Consistent with the leakiness observed in K15CREPR/RosaYFP mice, all untreated K15CREPR/$KRas^{LSL\text{-}G12D}$ mice eventually developed some papillomas, although the latency was increased in untreated mice (>6 mo) (Fig. S1*S*). These tumors possessed all of the histological characteristics of benign papillomas, as demonstrated by the expression of K5 in the basal layers and K1 in the suprabasal layers (Fig. 1 *I–M* and Fig. S1 *M–R*), indicative of squamous differentiation. No sign of malignant transformation was observed in these mice up to 4 mo after $KRas^{G12D}$ expression. Altogether, these data indicate that bulge SCs and their HF progeny are competent to develop benign papillomas upon $KRas^{G12D}$ expression, but other genetic events are required to induce the development of invasive carcinomas.

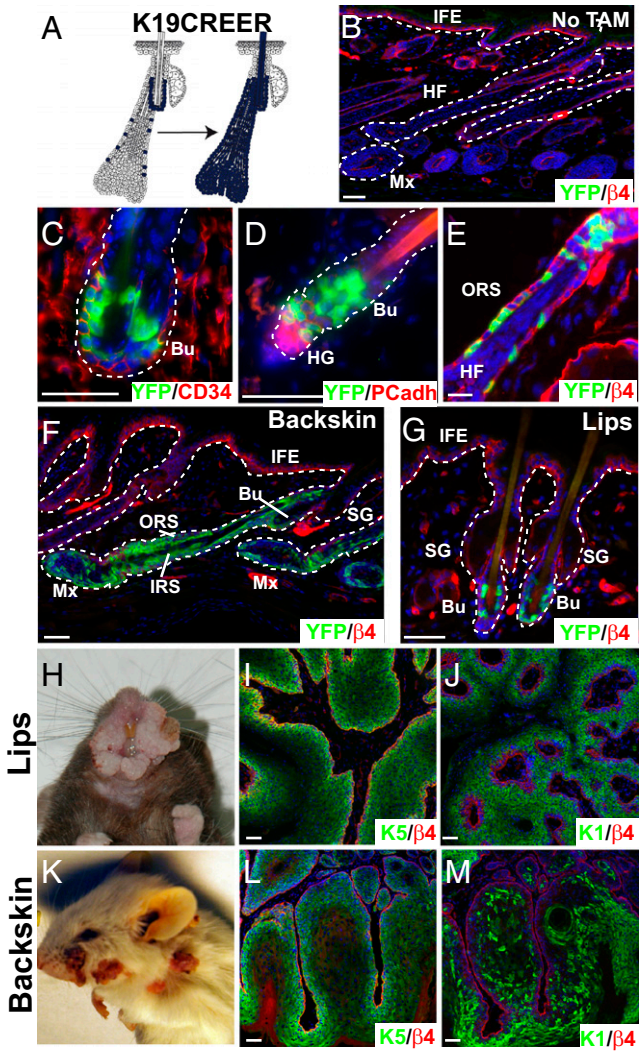

Fig. 1. Targeting $KRas^{G12D}$ expression in bulge SCs and their progeny induces papilloma formation. (*A*) Bulge SCs and their HF progeny targeted by *K19* promoter are highlighted in dark blue. (*B*) YFP immunostaining in the absence of TAM administration. (*C–G*) Lineage tracings of K19CREER/RYFP mice are shown in the bulge (*C*), HG (*D*), and ORS (*E* and *F*) of the back skin and in the bulge of the lips (*G*) 1 wk after 10 mg TAM administration. (*H–M*) Papilloma formation in K19CREER/$KRas^{LSL\text{-}G12D}$ mice. (*H* and *K*) Macroscopic pictures of tumors seen in the K19CREER/$KRas^{LSL\text{-}G12D}$ lips (*H*), face, and back skin (*K*) 4 mo after TAM administration. Expression of K5 (*I* and *L*) and of K1 (*J* and *M*) in papilloma from lips and back skin arising from K19CREER/$KRas^{LSL\text{-}G12D}$ mice. Bu, bulge; IRS, inner root sheath; Mx, matrix. (Scale bars, 50 μm.)

HF Transit Amplifying Cells Are Not Competent to Initiate Papilloma Formation upon KRas^{G12D} Expression. During HF regeneration, bulge SCs are activated, proliferate, and give rise to transit-amplifying (TA) cells, which differentiate into the hair shaft and its envelope (36). To determine whether KRas^{G12D} expression in HF TA compartment is sufficient to transform these cells and induce squamous tumor formation, we administered TAM to ShhCREER/KRas$^{LSL-G12D}$ mice at day 28 when HFs were in full anagen (Fig. 2*A*). No leakiness was detected in ShhCREER/RosaYFP mice (Fig. 2*B*). Administration of TAM to ShhCREER/RosaYFP mice preferentially labeled one side of the matrix. These labeled cells constitute a subset of matrix cells that differentiate into the different HF lineages (Fig. 2 *C*–*G*), showing that ShhCREER (37) activity is indeed restricted to the HF TA cells, as we previously described in the HF of the tail (31). Few marked YFP cells were still observed in the companion layer of the club hair 1 mo after TAM administration (Fig. S5*A*). RT-PCR analysis of FACS-isolated YFP cells from ShhCREER/RosaYFP demonstrated that *KRas* is expressed at a similar level in Shh-derived cells, in bulge SC, and in cells of the IFE and the infundibulum (Fig. S5*B*). Despite the similar level of *KRas* expression in matrix cells, no macroscopic tumors or microscopic HF or IFE defects (Fig. 2 *H*–*J* and Fig. S5 *C* and *D*) were observed in ShhCREER/KRas$^{LSL-G12D}$ mice 4 mo after TAM administration (n = 7), suggesting that KRas^{G12D} expression in HF TA cells is not sufficient to induce long-term renewal potential and initiate tumor formation.

KRas^{G12D} Expression in the IFE Induces Papilloma Formation. Transgenic mice expressing a mutated form of HRas under the promoter of *K10*, a keratin expressed in the suprabasal cells of the IFE, induced hyperkeratosis and papilloma formation in response to me-

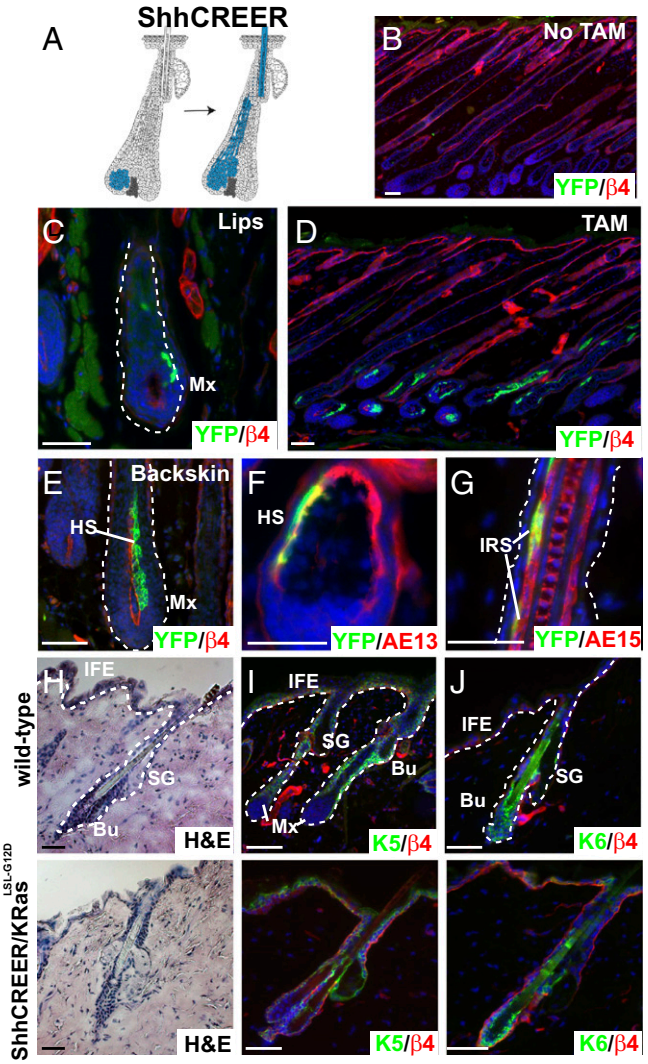

Fig. 2. Transit amplifying HF matrix cells do not give rise to papilloma upon KRas^{G12D} expression. (*A*) Matrix cells and their progeny targeted by *Shh* promoter are highlighted in blue. (*B*) YFP immunostaining in the absence of TAM administration. (*C*–*G*) Lineage tracing in ShhCREER/RYFP mice showed the presence of YFP cells in the matrix cells of the lips (*C*), HF (*D*), matrix (Mx), and hair shaft (HS) (*E* and *F*); inner root sheath (IRS) of the back skin (*G*) shows that ShhCREER marked TA matrix cells and their HF progeny 1 wk after 2.5 mg TAM administration. (*D*–*H*) Comparison between wild-type and ShhCREER/KRas$^{LSL-G12D}$ back skin 4 mo after 2.5 mg TAM administration. Hematoxylin-eosin staining (*H*) and expression of K5 (*I*) and K6 (*J*), (*H*) Oil-red-O staining in back skin, show no epidermal defect or tumor formation in mice expressing KRas^{G12D} in matrix cells. Bu, bulge; Mx, matrix. (Scale bars, 50 μm.)

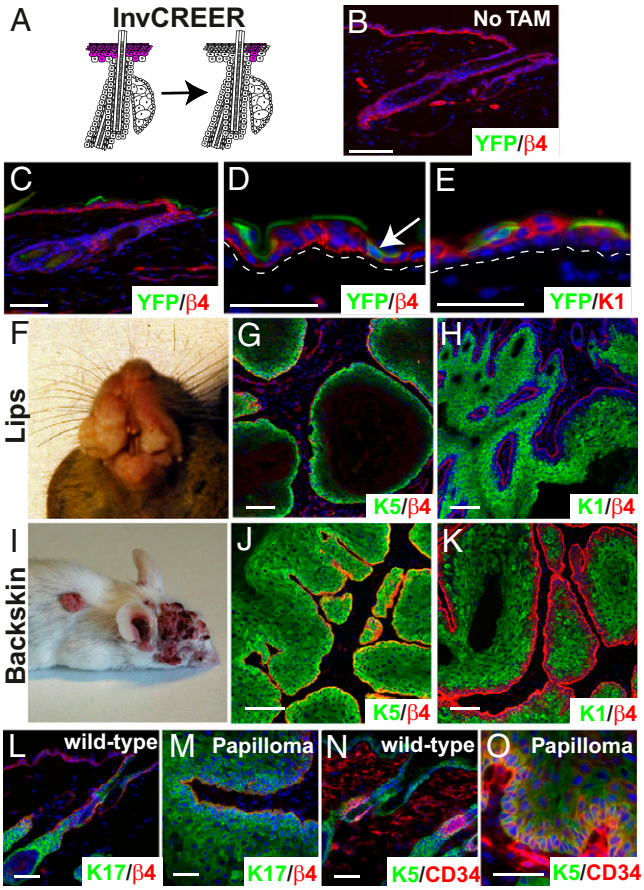

Fig. 3. KRas^{G12D} expression in the IFE induces papilloma formation. (*A*) Interfollicular suprabasal cells and rare basal cells targeted by *involucrin* promoter are highlighted in dark pink. (*B*) YFP immunostaining in the absence of TAM administration. (*C*–*E*) Lineage tracing of InvCREER/RosaYFP back skin mice 1 wk after 5 mg TAM administration. Costaining of YFP and β4, K5, and K1 shows that InvCREER mostly targets the suprabasal differentiated cells of the IFE, as well as some basal cells (*D*, arrow). (*F*–*K*) Papilloma formation in InvCREER/KRas$^{LSL-G12D}$ mice. (*F* and *I*) Macroscopic picture of tumors in the lips (*F*) and back skin (*I*) of InvCREER/KRas$^{LSL-G12D}$ mice 4 mo after TAM administration. Expression of K5 (*G* and *J*) and K1 (*H* and *K*) in papilloma from the back skin and lips of InvCREER/KRas$^{LSL-G12D}$ mice. (*L*–*O*) Follicular marker expression in papilloma arising from InvCREER/KRas$^{LSL-G12D}$ mice. Expression of K17 (*L* and *M*), a follicular marker, and CD34 (*N* and *O*), a bulge SC marker in wild-type epidermis (*L* and *N*) and papilloma (*M* and *O*) from InvCREER/KRas$^{LSL-G12D}$ mice, indicating that tumor differentiation does not reflect their cellular origin. (Scale bars, 50 μm.)

chanical stress (26). To determine whether physiological levels of KRas^{G12D} expression in the IFE can induce benign tumor formation during adult homeostasis, we generated transgenic mice expressing the TAM-inducible CREER in the suprabasal cells of the IFE. To this end, we generated transgenic mice expressing the CREERT2 under the human *involucrin* promoter (38) (InvCREER) (Fig. 3*A*). In the absence of TAM administration, no YFP cells was observed in InvCREER/RosaYFP, demonstrating the absence of leakiness of the InvCREER (Fig. 3*B*). Administration of TAM to InvCREER/RosaYFP mice resulted in the labeling of suprabasal cells of the IFE of the back skin and the lips (Fig. 3 *C–E*), although some basal cells (Fig. 3*D*) were also labeled in all three founders, consistent with the previous demonstration that ≈10% of basal cells already express markers of suprabasal cells (39). InvCREER also labeled some cells of the companion layer of the HF, as well as suprabasal cells of the infundibulum (Fig. S6*A*). After TAM administration in InvCREER/KRas$^{LSL\text{-}G12D}$ mice, recombination of *KRas^{G12D}* allele was detected in IFE cells (α6HCD34^{-}) but not in bulge SCs (α6HCD34H) (Fig. S6*B*). TAM administration in InvCREER/KRas$^{LSL\text{-}G12D}$ induced hyperthickening of the IFE (Fig. S6 *C–E*), with an increase in the number of layers expressing K5 (Fig. S6*E*), an increase in the proportion of cells expressing Ki67, and the expression of K6 (Fig. S6*C*). These data indicate that KRas^{G12D} expression in the IFE induced hyperproliferation and hyperplasia of the IFE. InvCREER/KRas$^{LSL\text{-}G12D}$ mice treated with TAM developed tumors in the lips (100% of the mice), face (40%), and back skin (80%) 2–4 mo after TAM administration (n = 5) (Fig. 3 *F* and *I*). Microscopic examination of these tumors demonstrated that they presented the hallmarks of benign papilloma with signs of squamous differentiation, as demonstrated by the expression of K1 and K5 (Fig. 3 *G–K*), and these tumors were indistinguishable from the papillomas obtained in K15CREPR/KRas$^{LSL\text{-}G12D}$ and K19CREER/KRas$^{LSL\text{-}G12D}$ mice. It has been recently shown that benign papillomas and invasive SCCs contained cancer SCs expressing CD34, a marker of bulge SCs, suggesting that squamous tumors may arise from bulge SCs (40). Interestingly, papillomas arising from the IFE of InvCREER/KRas$^{LSL\text{-}G12D}$ mice also express CD34 and K17, another follicular marker (Fig. 3 *L–O*), indicating that expression of HF markers by tumor cells does not necessarily reflect their cellular origin. None of these mice developed invasive carcinoma within the 4 mo after TAM administration. These results demonstrate that different cell lineages of the skin epidermis, including HF SCs and their progeny, as well as cells of the IFE, are competent to develop benign papillomas upon physiological KRas^{G12D} expression with similar latency and without the need of stimulation caused by injury.

Combined Expression of KRas^{G12D} and p53 Deletion in Epidermal Cells Is Necessary to Initiate SCC. Because no malignant tumor was observed in mice expressing KRas^{G12D} in any of the epidermal compartments tested and because *p53* gene dosage has been reported to control malignant progression in DMBA/TPA-induced skin tumors (41), we tested whether p53 deletion can promote the formation of invasive SCC in skin expressing KRas^{G12D}. To this end, we first determined whether KRas^{G12D} expression and p53 deletion in the epidermis are sufficient to initiate invasive SCC. We administered 1 mg TAM to K14CREER/KRas$^{LSL\text{-}G12D}$/p53$^{fl/fl}$ mice (Fig. 4*A*). At this dose, TAM administration in K14CREER/RosaYFP induced the expression of YFP in a mosaic manner in all epidermal compartments of the skin epidermis (31). TAM administration induced KRas^{G12D} expression and p53 deletion in K14CREER/KRas$^{LSL\text{-}G12D}$/p53$^{fl/fl}$ mice (Fig. S7). Within less than 2 mo they developed rapidly growing ulcerative lesions in the back skin (Fig. 4*B*) (n = 12). These ulcerative lesions represented invasive SCCs characterized by a fibroblast-like shape, expressed K5 but not K1 (Fig. 4 *C–G*), displayed disruption of basal lamina (Fig. 4*H*), and expressed markers of epithelial to mesenchymal transition (Fig. 4*I*). In addition to the macroscopic visible ulcerative lesions, many microscopic and small invasive SCCs were also observed in the dermis of the back skin (Fig. 4 *E–I*). These results

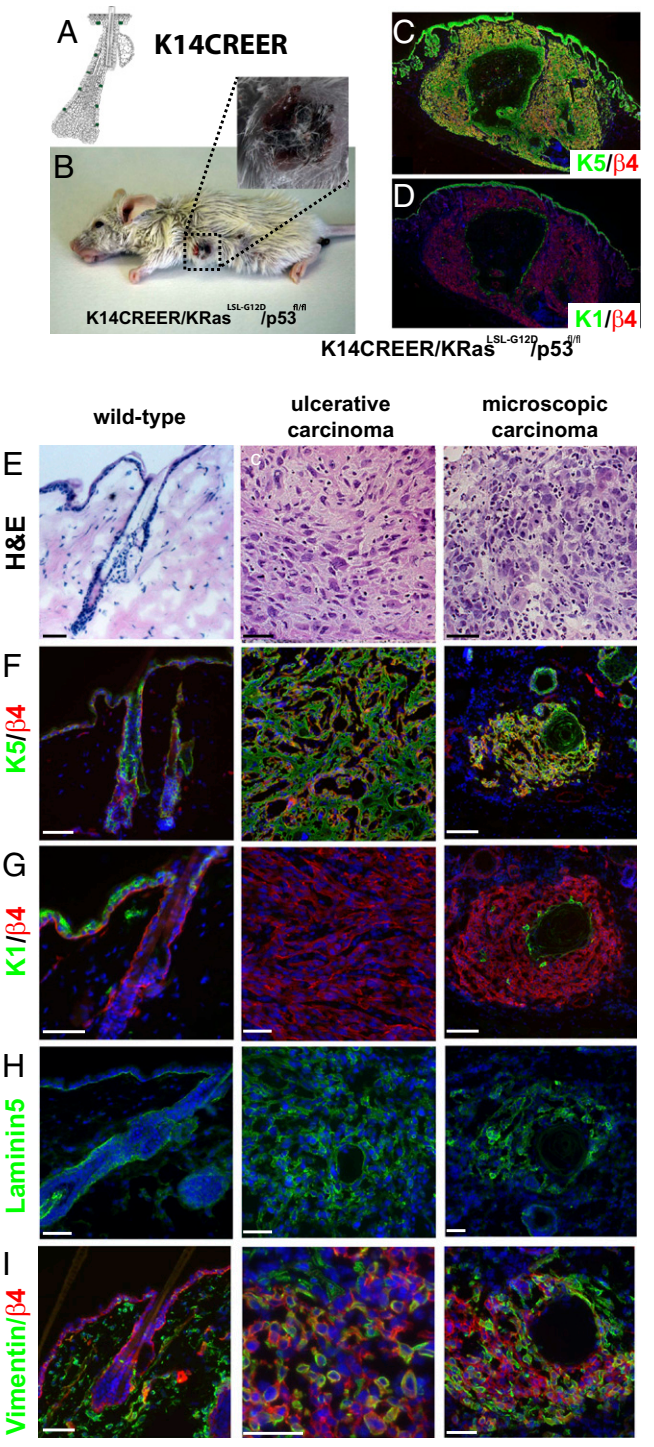

Fig. 4. Combined KRas^{G12D} expression and p53 deletion in the skin epidermis induces SCC. (*A*) IFE and HF basal cells targeted by *K14* promoter at clonal induction are highlighted in dark green. (*B*) Macroscopic picture of ulcerative back skin lesions from K14CREER/KRas$^{LSL\text{-}G12D}$/p53$^{fl/fl}$ mouse 1 mo after TAM administration. (*C* and *D*) Immunostaining of K5 (*C*) and K1 (*D*) in K14CREER/KRas$^{LSL\text{-}G12D}$/p53$^{fl/fl}$ back skin tumors show the absence of K1 expression in these tumors. (*E–I*) Comparison between wild-type back skin and SCC from K14CREER/KRas$^{LSL\text{-}G12D}$/p53$^{fl/fl}$ mice. Hematoxylin-eosin staining (*E*), expression of K5 (*F*), K1 (*G*), laminin5, a basal lamina marker (*H*), and vimentin, a mesenchymal marker (*I*), showing that these tumors present all histological and biochemical characteristics of invasive SCC. (Scale bars, 50 μm.)

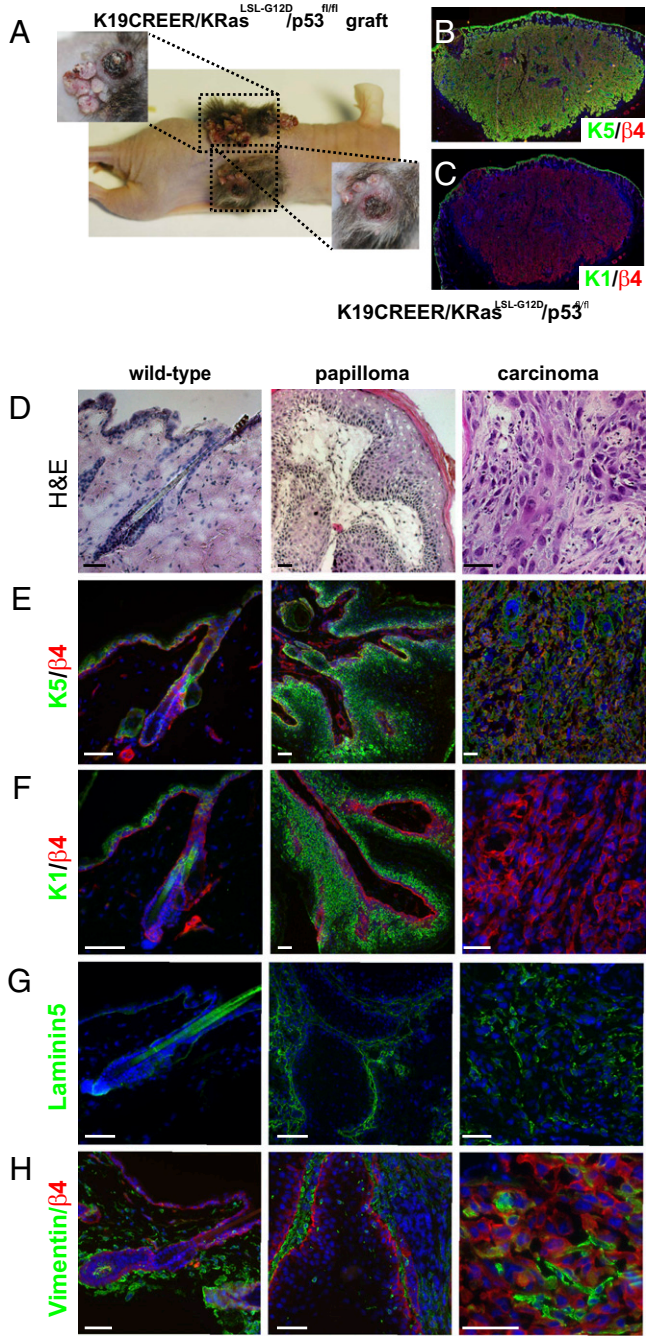

Fig. 5. KRas^{G12D} expression and p53 deletion in bulge SCs and their HF progeny induce SCC. (*A*) Macroscopic picture of tumors arising in K19CREER/KRas$^{LSL\text{-}G12D}$/p53$^{fl/fl}$ back skin grafted onto nude mouse. Immunostaining of K5 (*B*) and K1 (*C*) in K19CREER/KRas$^{LSL\text{-}G12D}$/p53$^{fl/fl}$ carcinoma. (*D–H*) Comparison between wild-type back skin, papilloma, and carcinoma arising from grafted K19CREER/KRas$^{LSL\text{-}G12D}$/p53$^{fl/fl}$ back skin. Hematoxylin-eosin staining (*D*) and expression of K5 (*E*), K1 (*F*), laminin5 (*G*), and vimentin (*H*) in wild-type back skin and in papilloma and SCC from K19CREER/KRas$^{LSL\text{-}G12D}$/p53$^{fl/fl}$ mice. (Scale bars, 50 μm.)

demonstrate that, in the context of oncogenic KRas, at least two genetic hits (gain of Ras and loss of p53 function) are required for the development of invasive carcinoma.

We then determined more specifically whether the expression of KRas^{G12D} combined with the p53 deletion in HF bulge SCs and their progeny also led to invasive SCC. To this end, we administered TAM to K19CREER/KRas$^{LSL\text{-}G12D}$/p53$^{fl/fl}$ mice, which specifically induce KRas^{G12D} expression and p53 deletion in bulge SCs and their progeny (Fig. S7). However, these treated mice died within 2 mo after TAM administration from intestinal cancers before developing skin tumors (n = 8). To circumvent this issue, we grafted the back skin of K19CREER/KRas$^{LSL\text{-}G12D}$/p53$^{fl/fl}$ mice onto the back skin of nude mice one month after TAM administration. All mice grafted with the skin of TAM-treated K19CREER/KRas$^{LSL\text{-}G12D}$/p53$^{fl/fl}$ mice developed many skin tumors, including ulcerative lesions, within 2 mo after TAM administration (Fig. 5*A*) (n = 10 grafts). Microscopic examination revealed that the majority of these tumors were differentiated benign papillomas, as shown by K1 expression (Fig. 5 *C* and *F*), but some of them presented all of the characteristics of invasive SCC (Fig. 5 *D–H*), which were indistinguishable from the SCC observed in K14CREER/KRas$^{LSL\text{-}G12D}$/p53$^{fl/fl}$ mice. To determine whether the expression of KRas^{G12D} and the loss of p53 in matrix TA cells can induce skin tumor formation, we administered TAM to ShhCREER/KRas$^{LSL\text{-}G12D}$/p53$^{fl/fl}$ mice. As in ShhCREER/KRas$^{LSL\text{-}G12D}$ mice, no macroscopic or microscopic tumors (Fig. S8) were observed in ShhCREER/KRas$^{LSL\text{-}G12D}$/p53$^{fl/fl}$ treated mice up to 4 mo after TAM administration (n = 10). These data clearly showed that the combined expression of KRas^{G12D} and p53 deletion in bulge SCs and/or their HF progeny are required to induce full-blown invasive skin SCC, whereas TA matrix cells were not competent to initiate benign or malignant tumors.

Discussion

For most cancers, the precise identification of tumor-initiating cells remains elusive. We have recently demonstrated that upon oncogenic smoothened expression, basal cell carcinoma (BCC) arose most frequently from the IFE, whereas bulge SCs and their HF progeny were not competent to initiate BCC formation upon smoothened expression (31). In sharp contrast, KRas^{G12D} oncogene expression in bulge SCs and their HF progeny gave rise to benign papillomas, and KRas^{G12D} expression combined with p53 deletion in these cells led to invasive SCC. Because K15 and K19 inducible CRE lines also targeted cells located within the HG and the lower ORS, we cannot exclude the possibility that some short-lived HF progenitors could be as potent as bulge SCs in initiating squamous tumors. In addition to bulge SCs, cells of the IFE are also competent to give rise to benign squamous tumors upon physiological expression of KRas^{G12D} oncogene without the need of exogenous inflammation or stimulation of tissue turnover by chemical abrasion or wounding. These data show that in contrast to the restricted epidermal lineages competent to initiate BCC upon smoothened expression (31), multiple epidermal compartments of the epidermis, but not matrix HF TA cells nor their hair shaft progeny, are competent to initiate squamous tumors upon KRas^{G12D} expression. The absence of tumor formation upon KRas^{G12D} expression in HF TA cells could be related to the transient period during which matrix cells actively proliferate. Indeed, it takes approximately 1 mo to detect the first microscopic lesions after KRas^{G12D} expression in HF or IFE progenitors, and after 1 mo the lower part of the HF has degenerated during catagen stage, and only rare Shh-derived cells are still present within the HF, as terminally differentiated cells.

Papillomas arising from bulge SCs targeted by KRas^{G12D} expressed K1, whereas bulge SCs and their HF progeny do not express K1 during physiological conditions. Similarly, papilloma arising from KRas^{G12D} expression in the IFE expressed CD34, like papillomas from DMBA/TPA-treated mice (40), although in normal skin CD34 is specifically expressed by bulge SCs but not IFE cells (42, 43). These results indicated that the expression of differentiation markers by tumor cells does not necessarily reflect the cellular origin of squamous tumors. Similarly, oncogenic smoothened expression induced the expression of follicular markers in interfollicular progenitors during BCC initiation (31).

Whereas oncogenic smoothened expression drove the majority of targeted cells to invasive BCC (31), only a minor fraction of

$KRas^{G12D}$ targeted cells formed squamous tumors, suggesting that papilloma initiation could require other additional genetic and/or epigenetic modifications in addition to oncogenic Ras expression. Interestingly, simultaneous deletion of p53 and $KRas^{G12D}$ expression can initiate the formation of invasive SCC without first forming papilloma, suggesting that p53 loss might control SCC initiation, in addition to promoting tumor progression (41).

The mouse model of invasive SCC resulting from the expression of oncogenic KRas and p53 deletion in HF bulge SCs is likely to be relevant for human SCC because the same oncogenes (Ras and p53) are also implicated in the pathogenesis of human SCC (7, 8), and the histology of SCC found in our mouse model recapitulates the histology of human SCC. In addition, our findings, showing that squamous tumors arise from HF bulge SCs as well as from nonhairy epidermis, recapitulate the spectrum of locations of squamous tumors found in humans, such as hairy and nonhairy skin, oral cavity, head and neck, and esophagus.

Methods

Mice. K14CREER (44), ShhCREER (37), K15CREPR (12), K19CREER (30), Rosa-YFP (45), $KRas^{LSL\text{-}G12D}$ (28), and $p53^{fl/fl}$ mice (46) have been previously described. Generation of InvCREER mice and induction of CRE-mediated recombination are described in *SI Methods*.

Histology, Immunostaining, and Imaging. These were performed as previously described (31) and are detailed in *SI Methods*.

Skin Graft Protocol. Mice were anesthetized with a mixture of 5% xylazine and 10% ketamine in PBS. Back skin of 2-mo-old TAM-treated mice were removed and grafted onto the back skin of nude mice. Skin grafts were monitored for carcinoma formation.

Isolation of Keratinocytes, DNA and RNA Extraction, Real-Time RT-PCR, and PCR Analysis of Cre-Mediated Recombination.

These are described in *SI Methods*.

ACKNOWLEDGMENTS. We thank our colleagues who provided us with reagents and whose gifts are cited in the text. P.A.S. and C.B. are Researchers of Fonds de la Recherche Scientifique (FRS)/Fonds National de la Recherche Scientifique (FNRS), K.K.Y. is a research fellow of the Formation à la Recherche dans l'Industrie et l'Agriculture (FRIA), and G.L. is post-doctoral fellow of the FRS/FNRS. This work was supported by a career development award from the Human Frontier Science Program Organization, the program CIBLES of the Wallonia Region, a grant from the Fondation Contre le Cancer and the fond Gaston Ithier, a starting grant from the European Research Council, and the European Molecular Biology Organization (EMBO) Young Investigator Program.

1. Alam M, Ratner D (2001) Cutaneous squamous-cell carcinoma. *N Engl J Med* 344: 975–983.
2. Kemp CJ (2005) Multistep skin cancer in mice as a model to study the evolution of cancer cells. *Semin Cancer Biol* 15:460–473.
3. Quintanilla M, Brown K, Ramsden M, Balmain A (1986) Carcinogen-specific mutation and amplification of Ha-ras during mouse skin carcinogenesis. *Nature* 322:78–80.
4. Spencer JM, Kahn SM, Jiang W, DeLeo VA, Weinstein IB (1995) Activated ras genes occur in human actinic keratoses, premalignant precursors to squamous cell carcinomas. *Arch Dermatol* 131:796–800.
5. van der Schroeff JG, Evers LM, Boot AJ, Bos JL (1990) Ras oncogene mutations in basal cell carcinomas and squamous cell carcinomas of human skin. *J Invest Dermatol* 94: 423–425.
6. Sutter C, et al. (1993) ras gene activation and aberrant expression of keratin K13 in ultraviolet B radiation-induced epidermal neoplasias of mouse skin. *Mol Carcinog* 8:13–19.
7. Perez-Losada J, Balmain A (2003) Stem-cell hierarchy in skin cancer. *Nat Rev Cancer* 3: 434–443.
8. Owens DM, Watt FM (2003) Contribution of stem cells and differentiated cells to epidermal tumours. *Nat Rev Cancer* 3:444–451.
9. Caulin C, et al. (2007) An inducible mouse model for skin cancer reveals distinct roles for gain- and loss-of-function p53 mutations. *J Clin Invest* 117:1893–1901.
10. Blanpain C, Fuchs E (2009) Epidermal homeostasis: A balancing act of stem cells in the skin. *Nat Rev Mol Cell Biol* 10:207–217.
11. Tumbar T, et al. (2004) Defining the epithelial stem cell niche in skin. *Science* 303: 359–363.
12. Morris RJ, et al. (2004) Capturing and profiling adult hair follicle stem cells. *Nat Biotechnol* 22:411–417.
13. Ito M, et al. (2005) Stem cells in the hair follicle bulge contribute to wound repair but not to homeostasis of the epidermis. *Nat Med* 11:1351–1354.
14. Levy V, Lindon C, Harfe BD, Morgan BA (2005) Distinct stem cell populations regenerate the follicle and interfollicular epidermis. *Dev Cell* 9:855–861.
15. Jensen UB, et al. (2008) A distinct population of clonogenic and multipotent murine follicular keratinocytes residing in the upper isthmus. *J Cell Sci* 121:609–617.
16. Jensen KB, et al. (2009) Lrig1 expression defines a distinct multipotent stem cell population in mammalian epidermis. *Cell Stem Cell* 4:427–439.
17. Snippert HJ, et al. (2010) Lgr6 marks stem cells in the hair follicle that generate all cell lineages of the skin. *Science* 327:1385–1389.
18. Ghazizadeh S, Taichman LB (2001) Multiple classes of stem cells in cutaneous epithelium: A lineage analysis of adult mouse skin. *EMBO J* 20:1215–1222.
19. Clayton E, et al. (2007) A single type of progenitor cell maintains normal epidermis. *Nature* 446:185–189.
20. Levy V, Lindon C, Zheng Y, Harfe BD, Morgan BA (2007) Epidermal stem cells arise from the hair follicle after wounding. *FASEB J* 21:1358–1366.
21. Morris RJ (2000) Keratinocyte stem cells: Targets for cutaneous carcinogens. *J Clin Invest* 106:3–8.
22. Morris RJ, Fischer SM, Slaga TJ (1986) Evidence that a slowly cycling subpopulation of adult murine epidermal cells retains carcinogen. *Cancer Res* 46:3061–3066.
23. Morris RJ, Coulter K, Tryson K, Steinberg SR (1997) Evidence that cutaneous carcinogen-initiated epithelial cells from mice are quiescent rather than actively cycling. *Cancer Res* 57:3436–3443.
24. Argyris TS, Slaga TJ (1981) Promotion of carcinomas by repeated abrasion in initiated skin of mice. *Cancer Res* 41:5193–5195.
25. Owens DM, Romero MR, Gardner C, Watt FM (2003) Suprabasal alpha6beta4 integrin expression in epidermis results in enhanced tumourigenesis and disruption of TGFbeta signalling. *J Cell Sci* 116:3783–3791.
26. Bailleul B, et al. (1990) Skin hyperkeratosis and papilloma formation in transgenic mice expressing a ras oncogene from a suprabasal keratin promoter. *Cell* 62:697–708.
27. Brown K, Strathdee D, Bryson S, Lambie W, Balmain A (1998) The malignant capacity of skin tumours induced by expression of a mutant H-ras transgene depends on the cell type targeted. *Curr Biol* 8:516–524.
28. Tuveson DA, et al. (2004) Endogenous oncogenic K-ras(G12D) stimulates proliferation and widespread neoplastic and developmental defects. *Cancer Cell* 5:375–387.
29. Raimondi AR, Molinolo A, Gutkind JS (2009) Rapamycin prevents early onset of tumorigenesis in an oral-specific K-ras and p53 two-hit carcinogenesis model. *Cancer Res* 69:4159–4166.
30. Means AL, Xu Y, Zhao A, Ray KC, Gu G (2008) A CK19(CreERT) knockin mouse line allows for conditional DNA recombination in epithelial cells in multiple endodermal organs. *Genesis* 46:318–323.
31. Youssef KK, et al. (2010) Identification of the cell lineage at the origin of basal cell carcinoma. *Nat Cell Biol* 12:299–305.
32. Arnold I, Watt FM (2001) c-Myc activation in transgenic mouse epidermis results in mobilization of stem cells and differentiation of their progeny. *Curr Biol* 11:558–568.
33. Niemann C, Owens DM, Hülsken J, Birchmeier W, Watt FM (2002) Expression of DeltaNLef1 in mouse epidermis results in differentiation of hair follicles into squamous epidermal cysts and formation of skin tumours. *Development* 129:95–109.
34. Horsley V, et al. (2006) Blimp1 defines a progenitor population that governs cellular input to the sebaceous gland. *Cell* 126:597–609.
35. Demehri S, Turkoz A, Kopan R (2009) Epidermal Notch1 loss promotes skin tumorigenesis by impacting the stromal microenvironment. *Cancer Cell* 16:55–66.
36. Blanpain C, Fuchs E (2006) Epidermal stem cells of the skin. *Annu Rev Cell Dev Biol* 22: 339–373.
37. Harfe BD, et al. (2004) Evidence for an expansion-based temporal Shh gradient in specifying vertebrate digit identities. *Cell* 118:517–528.
38. Carroll JM, Romero MR, Watt FM (1995) Suprabasal integrin expression in the epidermis of transgenic mice results in developmental defects and a phenotype resembling psoriasis. *Cell* 83:957–968.
39. Schweizer J, Kinjo M, Fürstenberger G, Winter H (1984) Sequential expression of mRNA-encoded keratin sets in neonatal mouse epidermis: Basal cells with properties of terminally differentiating cells. *Cell* 37:159–170.
40. Malanchi I, et al. (2008) Cutaneous cancer stem cell maintenance is dependent on beta-catenin signalling. *Nature* 452:650–653.
41. Kemp CJ, Donehower LA, Bradley A, Balmain A (1993) Reduction of p53 gene dosage does not increase initiation or promotion but enhances malignant progression of chemically induced skin tumors. *Cell* 74:813–822.
42. Trempus CS, et al. (2003) Enrichment for living murine keratinocytes from the hair follicle bulge with the cell surface marker CD34. *J Invest Dermatol* 120:501–511.
43. Blanpain C, Lowry WE, Geoghegan A, Polak L, Fuchs E (2004) Self-renewal, multipotency, and the existence of two cell populations within an epithelial stem cell niche. *Cell* 118:635–648.
44. Vasioukhin V, Degenstein L, Wise B, Fuchs E (1999) The magical touch: Genome targeting in epidermal stem cells induced by tamoxifen application to mouse skin. *Proc Natl Acad Sci USA* 96:8551–8556.
45. Srinivas S, et al. (2001) Cre reporter strains produced by targeted insertion of EYFP and ECFP into the ROSA26 locus. *BMC Dev Biol* 1:4.
46. Jonkers J, et al. (2001) Synergistic tumor suppressor activity of BRCA2 and p53 in a conditional mouse model for breast cancer. *Nat Genet* 29:418–425.

Supporting Information

Lapouge et al. 10.1073/pnas.1012720108

SI Methods

Generation of InvCREER Mice. The CREERT2 fragment was amplified from the vector pCre-ERT2 (1) [kindly given by P. Chambon, Institut de Génétique et de Biologie Moléculaire et Cellulaire (IGBMC), Illkirch-Graffenstaden, France] using ERT2-specific primers including NotI restriction sites and Pfx platinum polymerase (Qiagen). After cloning into TOPOblunt vector (Invitrogen), the fragment was digested by NotI restriction enzyme and cloned into the vector 3700Inv-pL2 that contains the human *involucrin* promoter, the SV40 intron, the SV40 polyA signal (2) [kindly given by F. M. Watt (Cancer Research Institute, Cambridge, United Kingdom)]. The resulting Involucrin-CREERT2 fragment was microinjected into fertilized oocytes [performed by Younes Achouri from the UCL facility (Université catholique de Louvain, de Duve Institute, Brussels, Belgium)]. Transgenic founders were first identified by PCR. Expression profiles of the founders were screened with reporter Rosa-YFP mice. The transgenic founder used in this study was then crossed with $KRas^{LSL\text{-}G12D}$ and Rosa-YFP mice.

Primary Antibodies. The following primary antibodies were used: anti-K5 (rabbit, 1:2,000; Covance), anti-GFP (rabbit, 1:1,000; Molecular Probes), anti-GFP (chicken, 1:4,000; Abcam), anti-β4 (rat, 1:200; BD Pharmingen), anti-KI67 (rabbit, 1:600; Abcam), anti-K1 (rabbit, 1:2,000; Covance), anti-K10 (rabbit, 1:2,000; Covance), anti-K6 (rabbit, 1/30,000; Covance), anti-laminin5α (rabbit, 1:1,000; Abcam), anti-vimentin (rabbit, 1:200; Abcam), anti-CD34 (rat, 1:100; BD Pharmingen), anti-K17 (rabbit, 1:6,000; kindly given by Pierre Coulombe, John Hopkins University, Baltimore, MD), anti-MTS24 [rat, 1/500; kindly provided by Richard Boyd (Monash Immunology and Stem Cell, Monash University, Clayton, Australia)], and anti-SCD1 (goat, 1/500; Santa Cruz).

Isolation of Keratinocytes, DNA and RNA Extraction, Real-Time RT-PCR, and PCR Analysis of Cre-Mediated Recombination. Isolation of keratinocytes was performed as previously described (3). Briefly, back skins from K19CREER/$KRas^{LSL\text{-}G12D}$, Inv-CREER/$KRas^{LSL\text{-}G12D}$ K19CREER/$KRas^{LSL\text{-}G12D}$/$p53^{fl/fl}$ K14-CREER/$KRas^{LSL\text{-}G12D}$/$p53^{fl/fl}$ at 2 d after the last tamoxifen (TAM) administration and from wild-type mice were incubated overnight in trypsin/EDTA at 4 °C (Gibco-Invitrogen). After isolation of keratinocytes, immunostaining was performed using anti-CD34 (clone RAM34; BD Biosciences) followed by streptavidin-allophycocyanin (BD Biosciences) and FITC anti-α6-integrin (clone GoH3; BD Biosciences). Living cells expressing epidermal cells were gated by forward scatter, side scatter, and by negative staining for Hoechst and by expression of CD34 and α6-integrin. FACS analysis was performed using FACSAria and FACSDiva software (BD Biosciences).

Isolation of Shh-derived cells was performed by isolating YFP expressing cells after TAM administration to ShhCREER/RosaYFP mice. After 3 d of TAM administration (0.1–0.2 mg/d), back skin of P8 mice was removed and incubated in Dyspase II (0.5 mg) (Sigma) overnight at 4 °C. Next day, dermis were separated from epidermis, cut in small pieces, and digested in collagenase 1% (Sigma) at 37 °C for 45 min on a checking incubator. Hair follicles (HF) were then collected after three rounds of centrifugation at 4 °C, corresponding to 5 min at 100 × *g* and two times at 40 × *g*. Collected HF were digested at 37 °C for 20 min and collected for FACS after trypsin neutralization and 70 μm, 40 μm mesh filtering. Living YFP-expressing epidermal cells were gated by forward scatter, side scatter, negative for Hoechst staining, and by expression of YFP. FACS analysis was performed using FACSAria and FACSDiva software (BD Biosciences).

For DNA extraction, sorted cells were harvested directly in Dulbecco's phosphate buffered saline (DPBS) supplemented with 10% FCS, and cell pellets were collected after one wash step in DPBS. DNA extraction was then performed using the classical phenol/chloroform protocol. For RNA extraction, sorted cells were harvested directly in the lysis buffer provided by the manufacturer (Stratagen), and total RNA extraction and DNase treatment of samples were performed using the Absolutely RNA Microprep kit (Stratagen), according to the manufacturer's recommendations.

After RNA quantification, purified RNA was used to synthesize the first-strand cDNA using SuperscriptII (Invitrogen) and random hexamers (Roche). Quantitative PCR analyses were performed with 2 ng of cDNA reaction as template, using a Brilliant II Fast SYBR QPCR Master Green mix (Stratagen) and an Agilent Technologies Stratagene Mx3500P real-time PCR system. All primers were designed using Lasergene 7.2 software (DNAStar). Analysis of results was performed with Mxpro software (Stratagene). The entire procedure was repeated in two or three biologically independent samples. Results were presented as the ratio of KRas Ct over the β-actin Ct for each type of epidermal cells isolated. Error bars represent SD.

To assess Cre-mediated recombination of the $KRas^{LSL\text{-}G12D}$ allele, PCR was performed as described using primers and protocol available on the Jacks Lab Web site (http://web.mit.edu/jacks-lab/). To detect recombination of the *p53* floxed allele, PCR was performed as previously described (4).

Analysis of BrdU Incorporation by FACS. BrdU (50 mg/kg) was administered i.p. 2 h before animal killing. Isolation of skin keratinocytes was performed as previously described (1). Immunostaining was performed using anti-CD34 (clone RAM34; BD Biosciences) followed by streptavidin-allophycocyanin (BD Biosciences) and phycoerythrin (PE) anti-α6-integrin (clone GoH3; BD Biosciences). BrdU staining was performed using BrdU Flow kit (BD Biosciences). FACS analysis was performed using FACSCalibur and CellQuestPro software (BD Biosciences).

Primers Used for Real-Time PCR.

KrasF 5′-AGA GCG CCT TGA CGA TAC AGC-3′
KrasR 5′-AAA GCC CTC CCC AGT TCT CAT-3′
b-actinF 5′-ACCAACTGGGACGATATGGAGAAGA-3′
b-actinR 5′-TACGACCAGAGGCATACAGGGACAA-3′

1. Indra AK, et al. (1999) Temporally-controlled site-specific mutagenesis in the basal layer of the epidermis: Comparison of the recombinase activity of the tamoxifen-inducible Cre-ER(T) and Cre-ER(T2) recombinases. *Nucleic Acids Res* 27:4324–4327.
2. Carroll JM, Romero MR, Watt FM (1995) Suprabasal integrin expression in the epidermis of transgenic mice results in developmental defects and a phenotype resembling psoriasis. *Cell* 83:957–968.
3. Blanpain C, Lowry WE, Geoghegan A, Polak L, Fuchs E (2004) Self-renewal, multipotency, and the existence of two cell populations within an epithelial stem cell niche. *Cell* 118:635–648.
4. Meuwissen R, et al. (2003) Induction of small cell lung cancer by somatic inactivation of both Trp53 and Rb1 in a conditional mouse model. *Cancer Cell* 4:181–189.

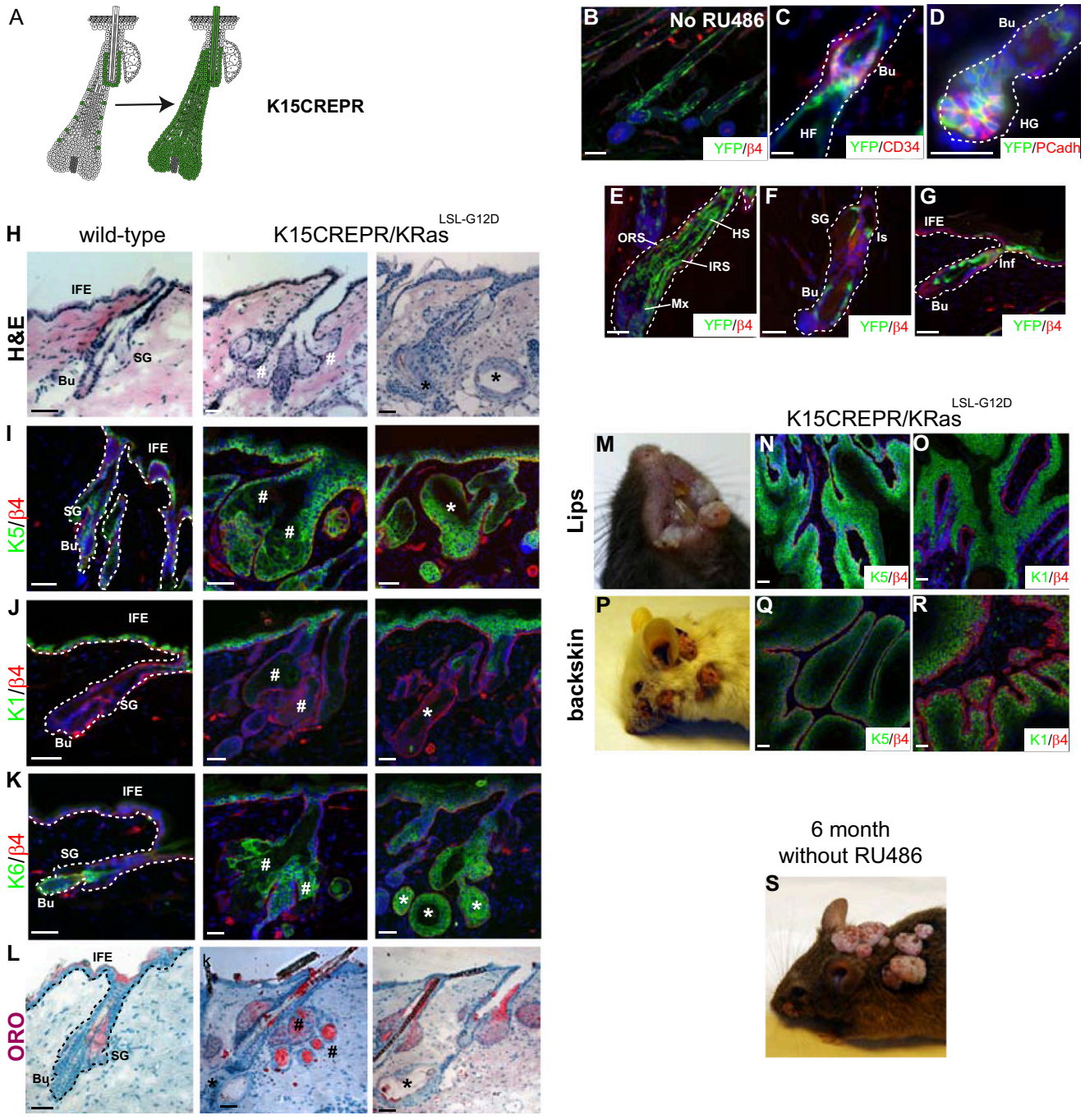

Fig. S1. Targeting KRas^{G12D} expression in bulge stem cells and their HF progeny using K15CREPR induces defects of sebaceous gland (SG) and HF differentiation and papilloma formation. (*A*) Bulge stem cells and theirs progenies targeted by the *K15* promoter are highlighted in dark green. (*B*) YFP immunostaining revealed the presence of YFP-positive cells in K15CREPR/RosaYFP in the absence of RU486 administration in 6-mo-old mice, indicating some leakiness in the K15CREPR mice. (*C*–*G*) YFP-positive cells targeted by the K15CREPR 7 d after RU486 administration: bulge cells (*C*), hair germ (HG) (*D*), outer root sheath (ORS) (*E*), isthmus (*F*), and interfollicular epidermis (IFE) (*G*). (*H*–*L*) Comparison of wild-type and K15CREPR/KRas$^{LSL-G12D}$ back skin 4 mo after RU486 administration. Defects of SG homeostasis leading to SG hyperplasia and cyst formation are shown in the middle column, whereas defects of HF differentiation and cysts are shown in the right column. (*H*) Hematoxylin-eosin staining. (*I*–*L*) Expression of K5 (*I*), K1 (*J*), K6 (*K*), and Oil-red-O (*L*) staining are shown. Macroscopic picture of tumor in the K15CREPR/KRas$^{LSL-G12D}$ lips (*M*) and back skin (*P*) 4 mo after RU486 administration. Expression of K5 (*N* and *Q*) and of K1 (*O* and *R*) in papilloma from lips and back skin arising in K15CREPR/KRas$^{LSL-G12D}$ mice. (*S*) Macroscopic picture of papillomas arising in 6-mo-old K15CREPR/KRas$^{LSL-G12D}$ mice in the absence of RU486 administration. Bu, bulge; HS, hair shaft; Inf, infundibulum; Is, isthmus; IRS, inner root sheath; Mx, matrix. *Follicular cysts; #sebaceous cysts. (Scale bars, 100 μm.)

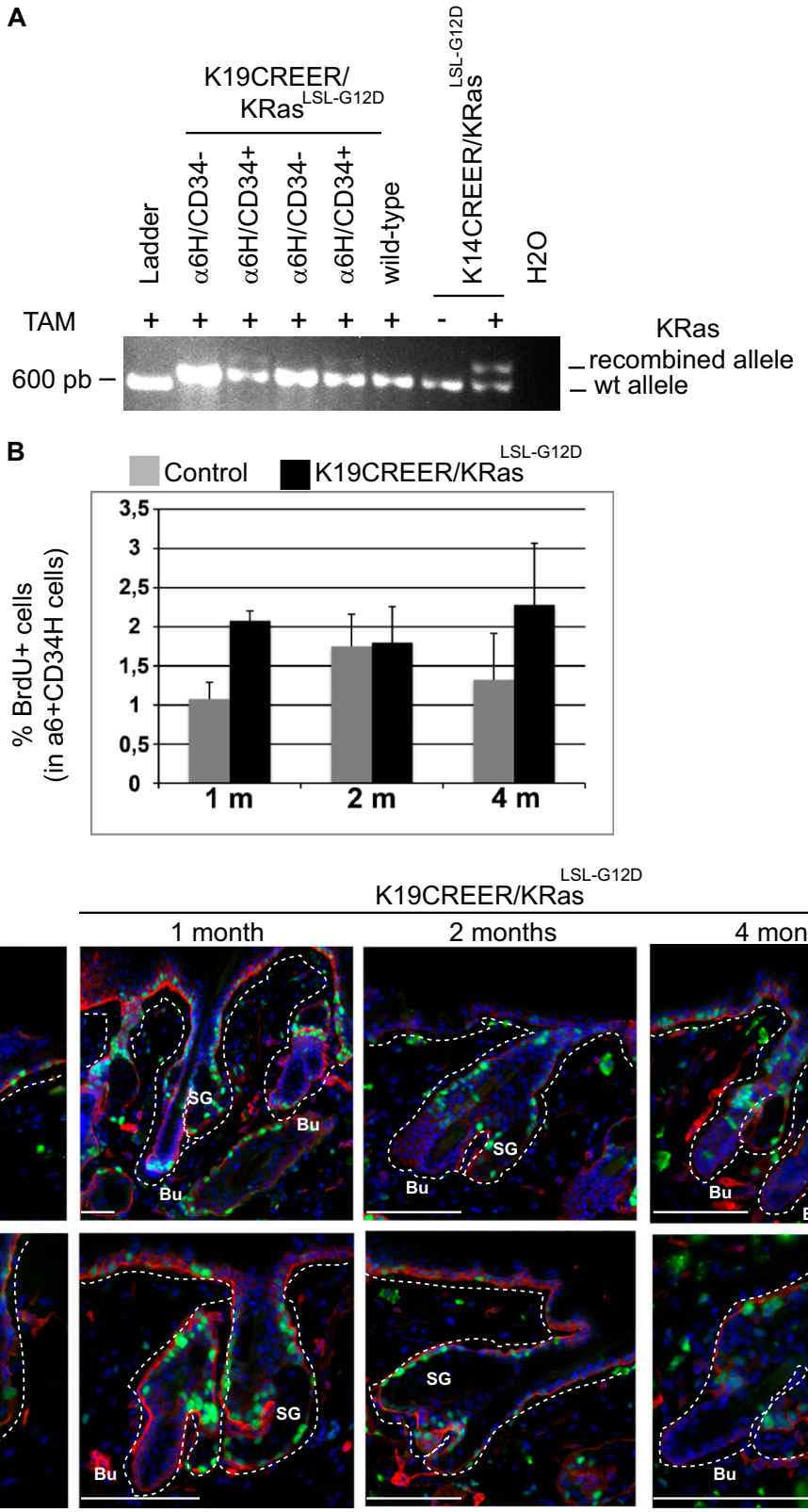

Fig. S2. Analysis of *KRas*^{G12D} recombination in bulge and sebaceous gland proliferation at different times after TAM administration in K19CREER/KRas$^{LSL\text{-}G12D}$ mice. (*A*) PCR analysis of *KRas*^{G12D} allele recombination 2 d after TAM administration in FACS-isolated bulge cells (α6HCD34H) and cells of the interfollicular epidermis and infundibulum (α6HCD34^{-}). (*B*) FACS quantification of BrdU-positive cells in bulge cells (α6HCD34H) of wild-type (gray bars) and K19CREER/KRas$^{LSL\text{-}G12D}$ (black bars) mice 4 h after BrdU administration. (*C*) Analysis of cell proliferation (Ki67) in wild-type and K19CREER/KRas$^{LSL\text{-}G12D}$ mice at 1, 2, and 4 mo after TAM administration. Bu, bulge; SG, sebaceous glands. (Scale bars, 100 μm.)

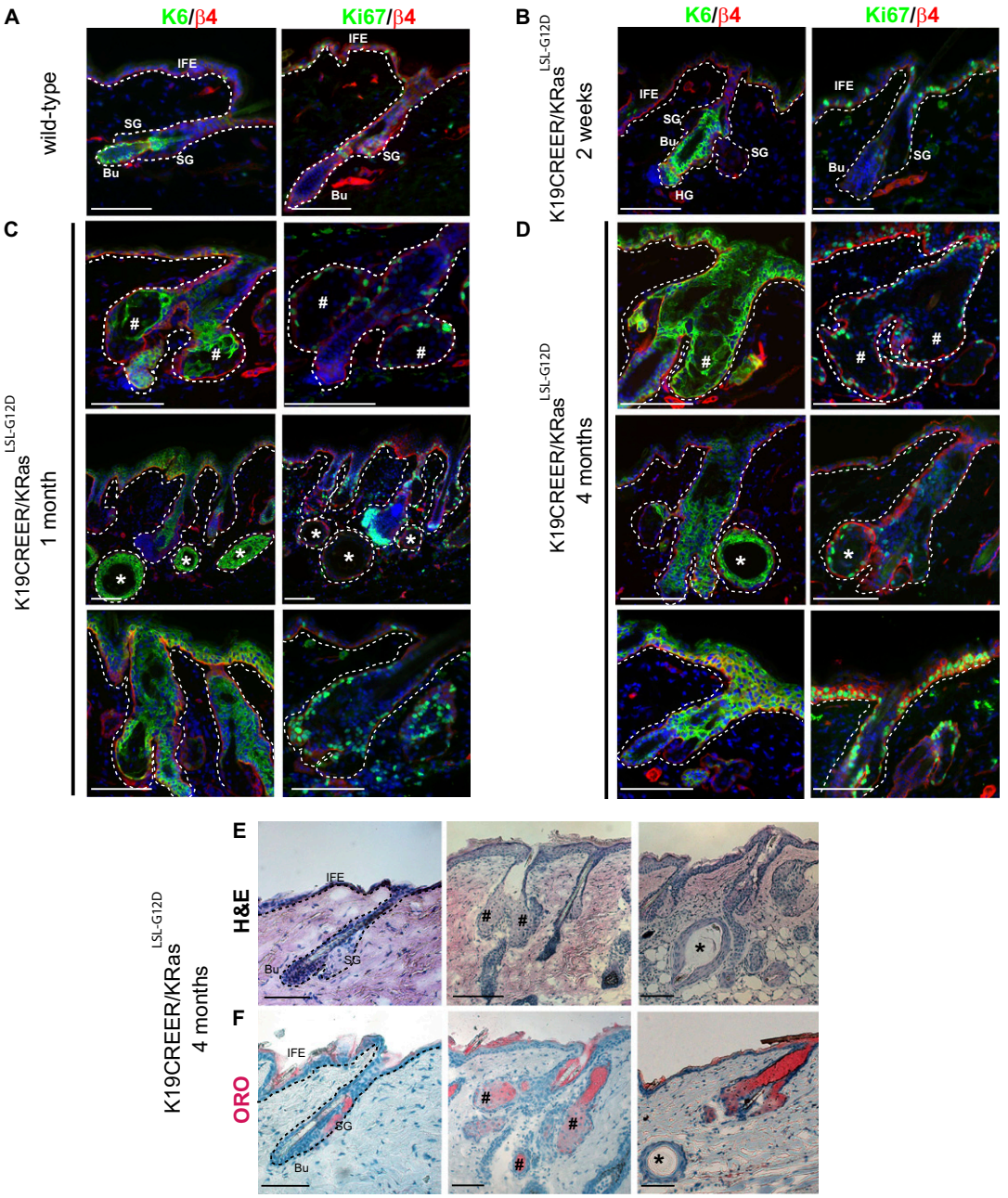

Fig. S3. Defect of sebaceous gland (SG) and HF differentiation leading to cystic formation after KRas^{G12D} expression in K19CREER/KRas$^{LSL\text{-}G12D}$ mice. (*A–D*) K6 and Ki67 expression in wild-type (*A*) and K19CREER/KRas$^{LSL\text{-}G12D}$ back skin at 2 wk (*B*), 1 mo (*C*), and 4 mo (*D*) after 10 mg TAM administration. Hematoxylin-eosin staining (*E*) and Oil-red-O (*F*) staining show hyperplasia and defect of SG and HF differentiation leading to cystic structures in the back skin of K19CREER/KRas$^{LSL\text{-}G12D}$ mice 4 mo after TAM administration.

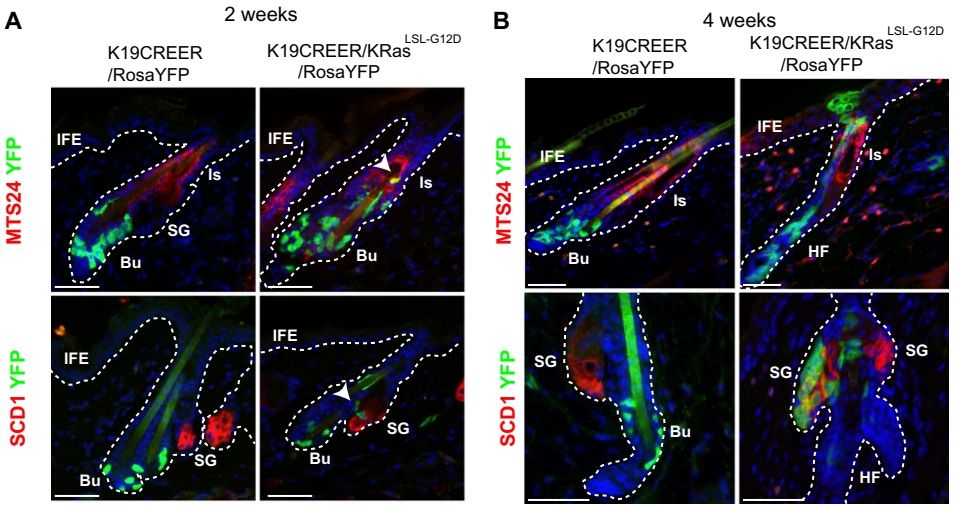

Fig. S4. Upward migration of K19 targeted cells in K19CREER/KRas$^{LSL-G12D}$/RosaYFP mice. (*A*) YFP-positive cells are detected in the isthmus (Is) (MTS24) compartment and in the sebaceous gland (SG) (SCD1) compartment at 2 wk after TAM administration in K19CREER/KRas$^{LSL-G12D}$/RosaYFP mice, whereas no YFP-positive cell was observed in the SG of K19CREER/RosaYFP mice. (*B*) At 4 wk after TAM administration, some YFP-positive cells have migrated throughout the infundibulum and have reached the interfollicular epidermis (IFE) in some regions of the back skin of K19CREER/KRas$^{LSL-G12D}$/RosaYFP, whereas no YFP-positive cell was observed in the IFE of K19CREER/RosaYFP mice. Bu, bulge. (Scale bars, 100 μm.)

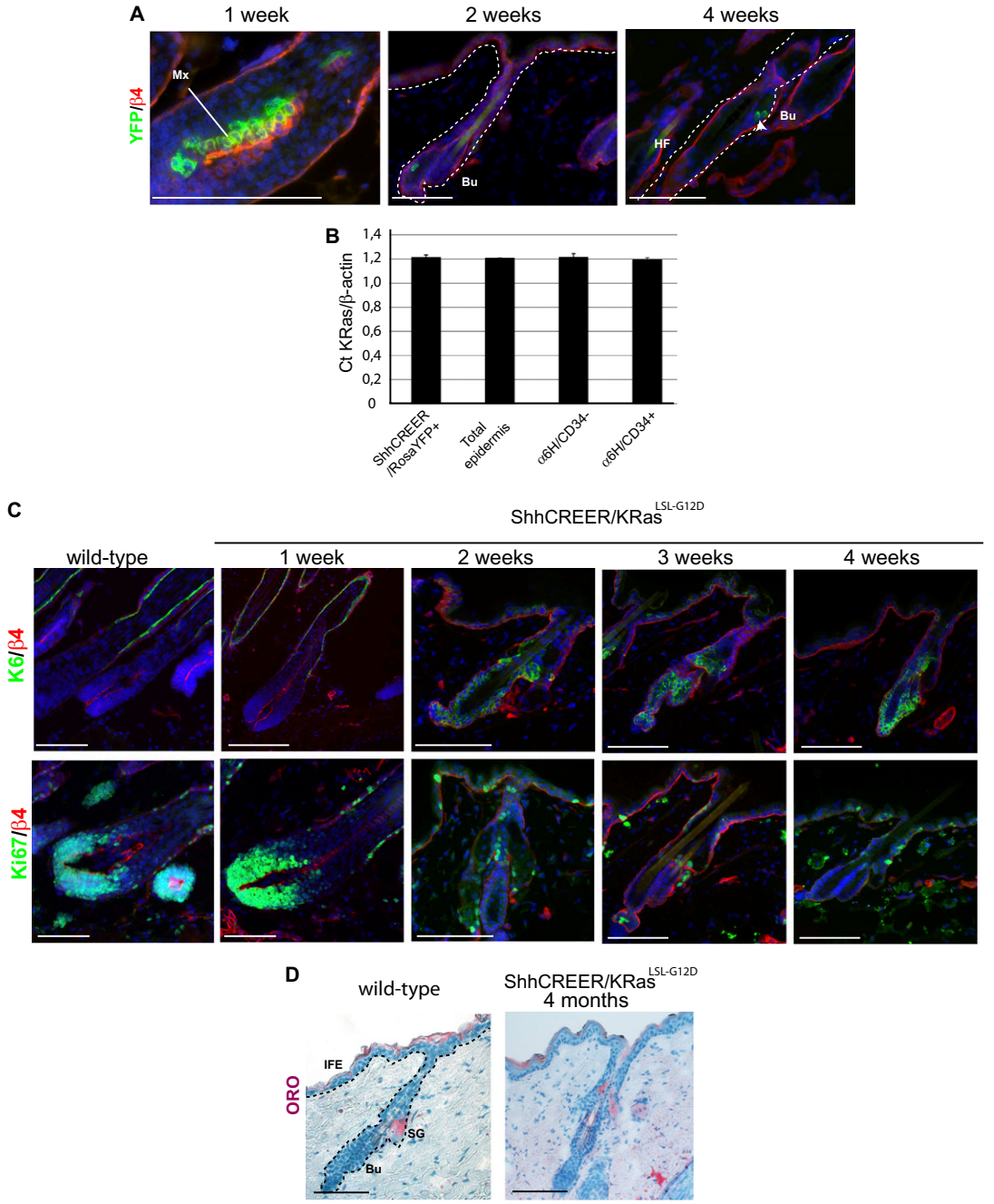

Fig. S5. ShhCREER lineage tracing, Ras expression, and phenotypic analysis after KRas^{G12D} expression in ShhCREER–derived cells. (*A*) YFP-positive cells are detected in the HF matrix and their progeny 1 wk after TAM administration, whereas 2 and 4 wk after TAM administration, only rare YFP cells were still detected in the differentiated companion layer cells of the HF. (*B*) RT-PCR analysis of *KRas* expression in FACS-isolated YFP cells from ShhCREER/RosaYFP mice 1 d after TAM administration, total epidermis (α6H+), bulge cells (α6HCD34H), cells of the interfollicular epidermis (IFE) and infundibulum (α6HCD34^{-}), showing similar level of *KRas* expression in the different epidermal compartments. (*C*) K6 (*Upper*) and Ki67 (*Lower*) expression in wild-type and ShhCREER/KRas$^{LSL-G12D}$ back skin at 1, 2, 3, and 4 wk after TAM administration. (*D*) Oil-red-O (ORO) staining in wild-type and ShhCREER/KRas$^{LSL-G12D}$ back skin 4 mo after TAM administration. Mx, matrix; Bu, bulge; SG, sebaceous gland. (Scale bars, 100 μm.)

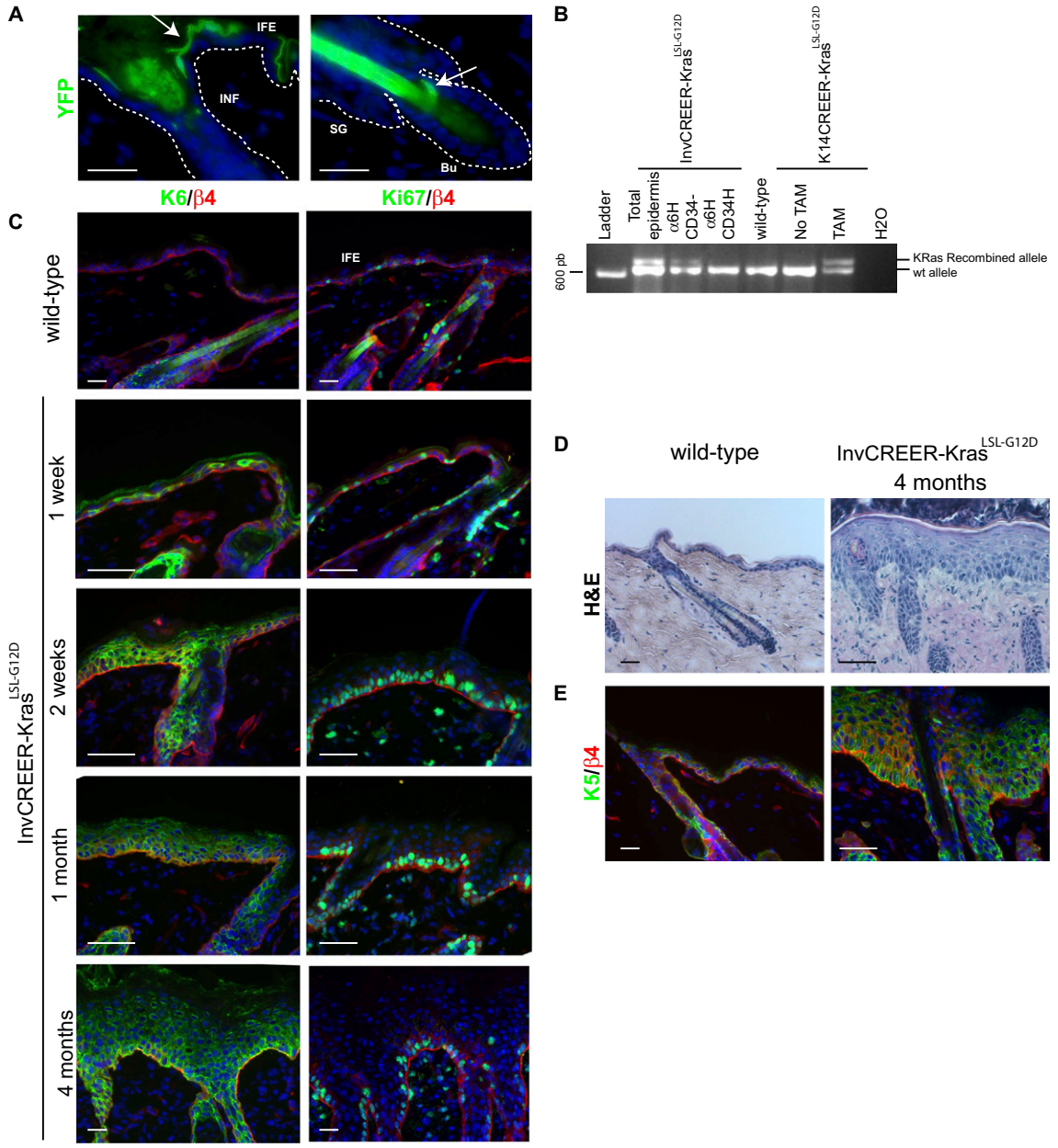

Fig. S6. Temporal analysis of cell proliferation and interfollicular epidermis hyperplasia after KRas^{G12D} expression in InvCREER/KRas$^{LSL\text{-}G12D}$ mice. (*A*) Lineage tracing 1 wk after TAM administration in InvCREER/RosaYFP mice, showing that some YFP-positive cells (arrows) can also be found in suprabasal cells of the infundibulum (INF) and in companion layer of the HF. IFE, interfollicular epidermis. (*B*) PCR analysis of *KRas^{G12D}* recombination after TAM administration in IFE and bulge cells of InvCREER/KRas$^{LSL\text{-}G12D}$ mice. (*C*) K6 (*Right*) and Ki67 (*Left*) expression in wild-type and InvCREER/KRas$^{LSL\text{-}G12D}$ back skin 1 and 2 wk and 1 and 4 mo after TAM administration. (*D* and *E*) Hematoxylin-eosin staining (*D*) and basal marker expression (K5/β4) (*E*) in wild-type and InvCREER/KRas$^{LSL\text{-}G12D}$ mice 4 mo after TAM administration show IFE hyperplasia upon KRas^{G12D} expression. (Scale bars, 50 μm.)

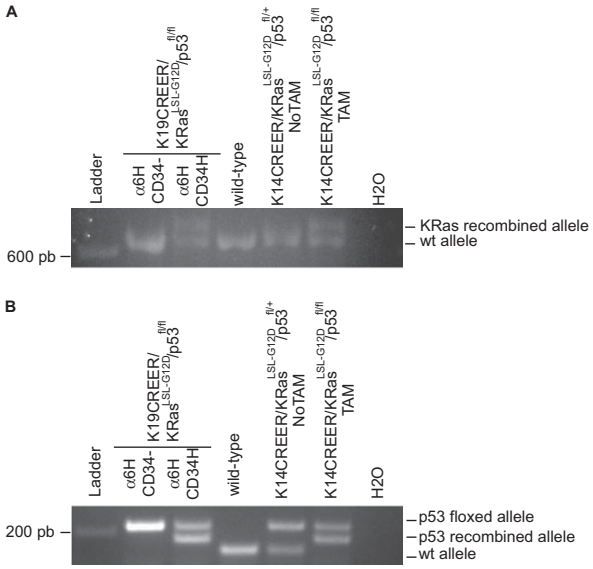

Fig. S7. PCR analysis of recombination of *KRas*^{G12D} and *p53* conditional alleles after TAM administration in K14CREER/KRas$^{LSL\text{-}G12D}$/p53$^{fl/fl}$ and in K19CREER/KRas$^{LSL\text{-}G12D}$/p53$^{fl/fl}$ mice. (*A*) PCR analysis of *KRas*^{G12D} recombination. (*B*) PCR analysis of *p53* recombination.

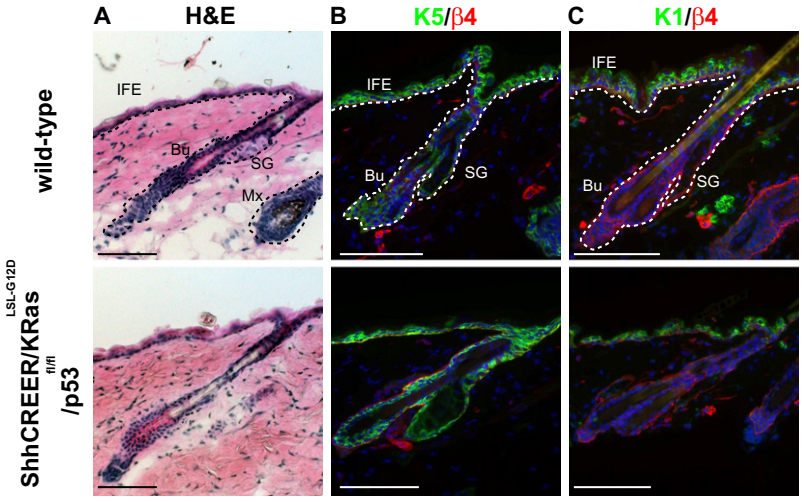

Fig. S8. Expression of KRas^{G12D} combined with the loss of p53 in HF matrix does not lead to tumor formation. ShhCREER/KRas$^{LSL\text{-}G12D}$/p53$^{fl/fl}$ mice were treated with 2.5 mg of TAM, and back skin was analyzed 4 mo later. (*A*–*C*) Hematoxylin-eosin staining (*A*) and expression of K5 (*B*) and K1 (*C*) in wild-type and 4 mo after TAM administration in ShhCREER/KRas$^{LSL\text{-}G12D}$/p53$^{fl/fl}$ mice. Bu, bulge; IFE, interfollicular epidermis; SG, sebaceous gland. (Scale bars, 100 μm.)